Journal of Porous Materials (2020) 27:691–700
https://doi.org/10.1007/s10934-019-00852-5

A novel anionic surfactant as template for the development of hierarchical ZSM-5 zeolite and its catalytic performance

R. Sabarish[1] · G. Unnikrishnan[1]

Published online: 8 January 2020

Abstract
A novel hierarchical ZSM-5 zeolite was successfully prepared by utilizing soft mesotemplate by hydrothermal treatment. TPAOH was used as a structure directing agent to create micropores and anionic surfactant HDSS were used to generate additional mesopores in the zeolite framework. The synthesized catalysts were characterized by using XRD, FT-IR, ^{27}Al and ^{29}Si NMR, SEM, TEM, NH_3-TPD, TGA and N_2 adsorption methods. XRD and FT-IR analysis shows that the synthesized catalyst possesses pronounced crystallinity with characteristics MFI structure. Development of micro/mesoporosity in the samples was noted by SEM and is complementary to TEM and BET analysis. The thermal stability and acidity of the synthesized samples were confirmed by TGA and NH_3-TPD technique. Catalytic activity of the synthesized ZSM-5 zeolites was examined for the oxidation of benzyl alcohol in presence of hydrogen peroxide. The results reveal that the surfactant assisted samples offer higher conversion and selectivity compared to conventional zeolites.

Keywords ZSM-5 · mesoporous · surfactants · catalytic activity

1 Introduction

Benzaldehyde (BzH) is one of the useful compounds which have been extensively exploited by pharmaceutical, perfumery, food and dye industries. It is commercially synthesized from conventional approaches such as oxidation of toluene or hydrolysis of benzyl chloride. However, these approaches are associated with drawbacks such as low selectivity and chlorine contaminant BzH and thus are not suitable for bulk preparation of BzH [1–4]. It is previously reported that the liquid phase catalytic oxidation of benzyl alcohol with oxidants is more suitable to synthesis BzH [5]. Various inorganic oxidants such as MnO_2, pyridinium dichromate, Jones reagent etc. were successfully used as oxidant for carrying out oxidation reaction [6, 7]. Perhaps, in recent years the usage of these oxidant is limited in view of its toxic and expensive nature; leading to the precipitous increase in the utilization of green oxidant, hydrogen peroxide for oxidation reaction [8, 9]. Researchers have employed both homogeneous and heterogeneous catalysts for the liquid phase oxidation of benzyl alcohol with hydrogen peroxide. Much interest is given to the fabrication of heterogeneous catalyst in liquid phase reactions, owing to its several advantages such as ease of product recovery, reusability, less corrosion etc. [10–13].

ZSM-5 zeolites are porous, crystalline aluminosilicates with well-defined microporosity and tunable properties [14–19]. Presence of high acid centre and shape selective nature make it an attractive catalyst in organic synthesis especially in cracking reactions. They also find application as an adsorbents and ion-exchangers [20, 21]. Besides these conventional applications, zeolites have been recently exploited in various sustainable processes such as fuel cells [22], water purification [23], air pollution control [24], thermal energy [25] etc. It is known that zeolite exhibit better catalytic performance than conventional solid catalyst [26]. However, the small micropores in them restrict their utilization in reactions involving bulkier reactants. One promising approach to overcome this problem was the development of hierarchical zeolites. Wide range of porosity (micro/meso/macro) in hierarchical zeolite reduces the diffusion limitations of conventional microporous zeolite and thus promotes large molecular reaction [27, 28]. Two major strategies adopted to tailor the pore size of zeolite are top down (demetallization)

✉ G. Unnikrishnan
unnig@nitc.ac.in

[1] Department of Chemistry, National Institute of Technology, Calicut, Kerala 673601, India

and bottom up (hard/soft templating) methods. [29–31]. In demetallisation method either aluminium (dealumination) or silicon (desilication) is extracted from the zeolite framework by leaching or steaming. Although this method is widely employed to induce mesoporosity in zeolite, it often results in mass loss and decline the catalytic performance of zeolite. Hence considerable research has been devoted to templating method in which hard (carbon aerogel, carbon nanotubes, polystyrene bead, $CaCO_3$ etc.) or soft (surfactants, silytaled polymer etc.) mesotemplates were introduced to the reaction mixture and later removed by calcination or extraction to develop large pore zeolites [32–37].

Compared to hard templating method, soft templating method is a preferred approach as it possesses good compatibility with zeolite precursors, and offers the opportunity to tune the pore size by varying the amount of template [38–41]. Liu et al developed a mesoporous ZSM-5 using a gemini surfactant which acted as a structure directing agent as well as mesoporous directing template. The prepared mesoporous ZSM-5 catalyst exhibited good catalytic activity for the aldol condensation of benzaldehyde [42]. Vijaya et al. [26] employed non-ionic surfactant Triton X-100 to generate hierarchical zeolite. The synthesized catalyst exhibits superior catalytic performance than conventional zeolite for oxidation of benzyl alcohol. Xu and co-workers elucidated the synthesis of mesoporous ZSM-5 using CTAB, which acted as a structure directing agent [43]. Meanwhile, Hensen and co-workers reported excellent catalytic performance, for methanol to hydrocarbon conversion, using hierarchical ZSM-5 zeolite developed using cetyltrimethylammonium (CTA) hydroxide [44]. Recently, Zhu et al prepared hierarchical ZSM-5 nanosheets with intracrystal mesopores and honeycomb morphology in the presence of hexadecyl trimethyl ammonium bromide (CTAB) as a second template [45]. Only a few reports are available on anionic surfactant templated hierarchical zeolite. Recently, Gomez et al successfully utilized anionic surfactant sodium dodecylbenzenesulfonates (SDBS) as the template for the preparation of mesoporous zeolite and observed improved catalytic performance for deoxygenation reactions, which find application in upgrading biofuels processes [46, 47].

The present work highlights the synthesis of a hierarchical ZSM-5 catalyst using a novel anionic surfactant hexadecanesulfonic acid sodium salt (HDSS). The synthesized catalysts were characterized by XRD, FT-IR, SEM, TEM, N_2 adsorption isotherm, NH_3-TPD and ^{27}Al and ^{29}Si NMR. The catalytic performance of the synthesized catalyst was assessed using a large molecular reaction: oxidation of benzyl alcohol. The effects of amount of catalyst, reaction time, temperature and reusability of the catalyst on the conversion rate have also been investigated in detail.

2 Experimental

2.1 Materials

Tetrapropyl ammonium hydroxide [$(CH_3CH_2CH_2)_4NOH$; TPAOH], tetraethylorthosilicate ($C_8H_{20}O_4Si$; TEOS), aluminium isopropoxide ($C_9H_{21}AlO_3$; AIP) and hexadecanesulfonic acid sodium salt ($CH_3(CH_2)_{15}SO_3Na$, HDSS), were purchased from Sigma Aldrich Co. Ltd (India). Sodium hydroxide (NaOH), hydrogen peroxide (H_2O_2) and benzyl alcohol (C_7H_7OH) used were of reagent grade, procured from Merck, and were used without further purification.

2.2 Synthesis

Hierarchical ZSM-5 zeolite was synthesized by mixing 0.03 g of aluminium isopropoxide (AIP) and 2.11 g of tetrapropylammonium hydroxide (TPAOH). To the clear solution, 3.46 g of tetraethyl orthosilicate (TEOS), 0.15 g of NaOH and 7 mL of distilled water were added with stirring for 5–6 h. To the solution, 0.2 g of the surfactant was added and kept for stirring at room temperature. The solution was concentrated at 80 °C in a rotavapour for 20 min to get a transparent sticky solution. The resulting sol was transferred into an autoclave, and then kept in an oven at 80 °C for 24 h. The sample was later hydrothermally treated at 175 °C for 6 h. The obtained product was washed with deionized water, dried in air, and calcined at 550 °C for 5 h to remove the organic components. The sample obtained using surfactant as template has been denoted as ZSM-5/HDSS.

For comparison, we have synthesized another ZSM-5 sample using the same procedure but in the absence of surfactants which has been represented as ZSM-5.

2.3 Catalytic reaction

2.3.1 Oxidation of benzyl alcohol with H_2O_2

The catalytic oxidation of benzyl alcohol was carried out in a 50 mL R.B flask connected with a water condenser and thermometer. In a typical run, 0.06 g of catalyst, 10 mmol of benzyl alcohol, 15 mmol of 30% H_2O_2 were mixed with 10 mL acetonitrile and the resulting mixture was heated at 90 °C for 4 h. After the reaction, the product is centrifuged, washed and was analysed using a gas chromatograph with an FID detector and a Rtx@5 column (30 m × 0.25 mm × 0.25 µm) and nitrogen as the carrier gas.

2.4 Characterization

X-ray diffraction (XRD) patterns were obtained with a Rigaku Miniflex 2200 diffractometer using CuKα radiation. FT-IR spectrum was recorded at room temperature using an FT-IR spectrometer Jasco 4700 in the range of 400–4000 cm^{-1}. Scanning electron microscopic images were obtained by using a Hitachi SU6600 Variable Pressure Field Emission Scanning Electron Microscope (SEM). Transmission electron micrographs (TEM) were taken with a JEOL JEM-2100 transmission electron microscope operated at an accelerating voltage of 200 kV. Thermogravimetric (TG) analysis of the uncalcined zeolite samples (TG) was done using a TGA Instrument Q50 at a heating rate of 10 °C min^{-1} in nitrogen. BET surface area and pore size distributions were inspected by N_2 adsorption–desorption using a Micromeritics Gemini V-2380 surface area analyzer. MAS NMR spectra were recorded on a Bruker Avance AV 300 spectrometer. The temperature programmed desorption (TPD) patterns with ammonia on the samples were recorded on a Micromeritics Chemisorb 2750.

3 Results and discussion

3.1 XRD patterns

XRD patterns of the surfactant modified and unmodified ZSM-5 samples are shown in Fig. 1. The synthesized samples exhibited peaks at 2θ = 7.98°, 8.82°, 14.82°, 23.14°, 23.96° and 24.44° associated with [011], [020], [031], [051], [303] and [313] plane, which is characteristics of MFI

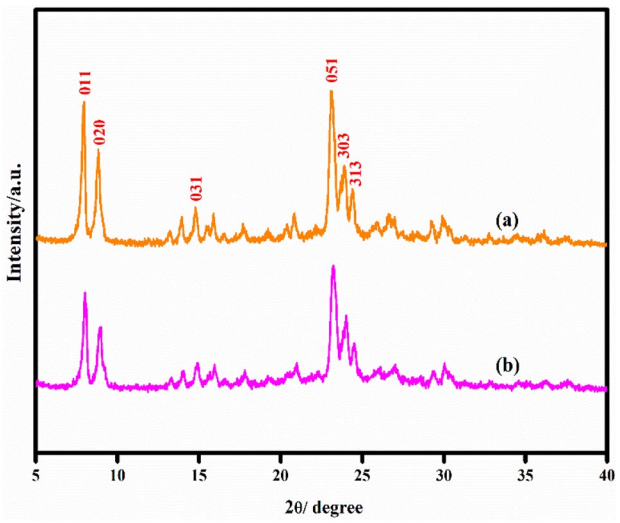

Fig. 1 XRD patterns of (a) ZSM-5, (b) ZSM-5/HDSS

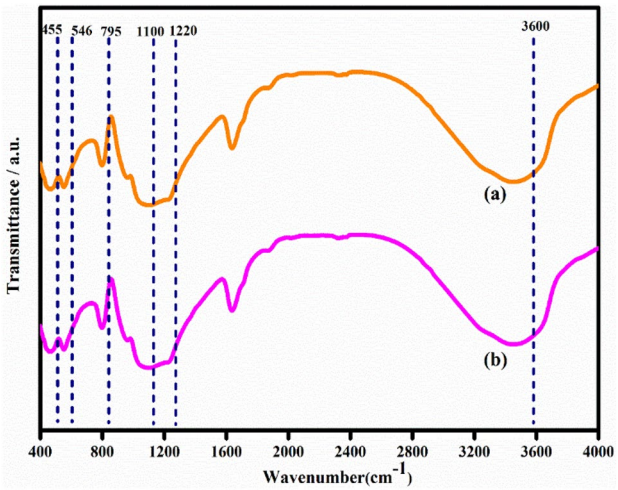

Fig. 2 FTIR spectra of (a) ZSM-5, (b) ZSM-5/HDSS

structure of ZSM-5 zeolite (JCPDS no. 42-0024) [48]. It is evident from Fig. 2, that the intensity of the characteristic peak in modified samples is comparable with unmodified samples indicating that the crystallinity of the sample is retained even after modification with surfactant.

3.2 3.2 FT-IR analysis

The FT-IR spectra of the surfactant modified and unmodified ZSM-5 recorded from 400 to 4000 cm^{-1} range is presented in Fig. 2. Absorption bands at 455 cm^{-1} (T–O bending), 795 cm^{-1} (external symmetric stretching), 1100 cm^{-1} (internal asymmetric stretching) and 1220 cm^{-1} (external asymmetric stretching) correspond to siliceous materials. The peak at 3600 cm^{-1} is attributed to the stretching frequency of isolated silanol groups, Si–O–H bond while the peak at 1630 cm^{-1} is attributed to adsorbed water. The band appears at 546 cm^{-1} corresponds to the double five-ring units present in pentasil zeolites [49].

3.3 ^{27}Al and ^{29}Si NMR

The local coordination environments of surfactant modified ZSM-5 zeolite were evaluated by ^{27}Al MAS and ^{29}Si NMR spectra (Fig. 3). ^{27}Al MAS spectra display an intense signal at δ = 54 ppm corresponding to the tetrahedral Al coordination. A weak signal appeared at ~0 ppm originates from the presence of extra-framework Al species, which is commonly reported in mesoporous zeolites [50, 51]. Meanwhile, the ^{29}Si NMR spectra of the sample show a major peak at − 113 ppm, corresponding to Si $(OSi)_4$ $(Q)^4$ and a weak shoulder peak at − 105 ppm due to $(AlO)_1$ Si-$(OSi)_3$ $(Q)^3$ respectively [52].

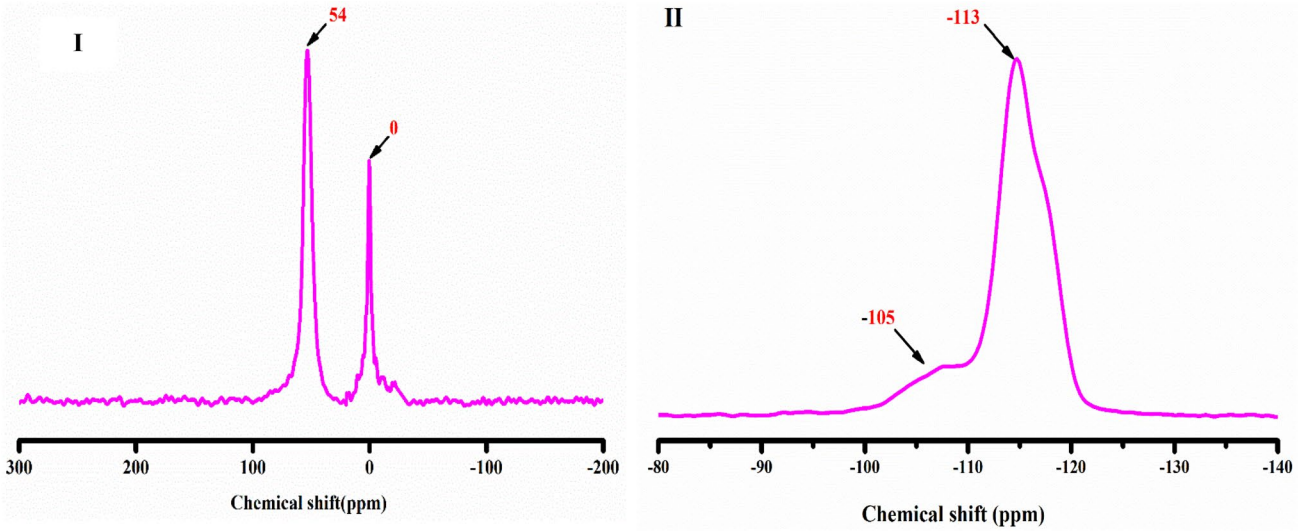

Fig. 3 **I** ^{27}Al and **II** ^{29}Si NMR spectra of ZSM-5/HDSS sample

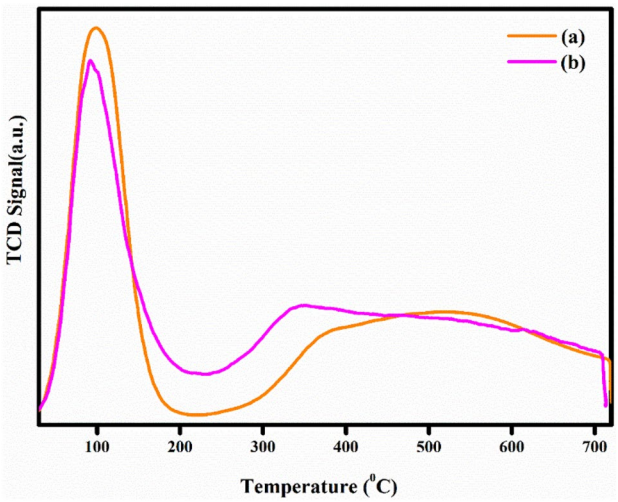

Fig. 4 NH_3-TPD profiles of: a ZSM-5, b ZSM-5/HDSS samples

3.4 NH_3 -TPD

The temperature programmed desorption of ammonia (NH_3-TPD) profiles of the surfactant modified and unmodified ZSM-5 samples are shown in Fig. 4. Both samples exhibit two desorption peaks: one at 300–400 °C (low temperature peak) and the second one at 500–700 °C (high temperature peak) respectively. The peak located at the low temperature region can be assigned to the desorption of NH_3 molecules from the weak acid sites, and the high temperature peak represents the strong acid sites. A slight decrease in the intensity of surfactant modified sample is attributed to the formation of mesoporosity in the framework [53–57]. TPD analysis thus suggests that HDSS is a suitable template for the development of hierarchical zeolite without significantly sacrificing the acidity of the zeolite.

A proposed mechanism for the formation of hierarchical ZSM-5 zeolite is shown in Scheme 1. Initially, the zeolite precursors along with surfactants are mixed at room temperature. During nucleation and crystallisation, the zeolite precursors gets transformed in to zeolite crystals; which get embedded in the surfactant micelles. Finally, the surfactants and organic templates were removed by calcination process, to generate meso and microporosity in the sample.

3.5 SEM and TEM

Scanning electron microscopic i.e. (SEM) and transmission electron microscopic i.e. (TEM) images provide information about the morphology of the synthesized catalyst as shown in Figs. 5 and 6 respectively. The HDSS modified zeolite possesses disc or quasi spherical morphology with rough surfaces and is in accordance with previous reported work [58, 59]. Agglomerated nano particle in the range of 100–400 nm diameters is also visible in the SEM image. TEM micrographs were complementary to SEM analysis and confirm the development of pores in the range of micro and meso dimensions (Fig. 6a–d). A selected-area electron diffraction (SAED) pattern of the corresponding ZSM-5 zeolites is also provided in the inset of Fig. 6d. The SAED pattern implies that the modified ZSM-5 samples possess good crystallinity.

3.6 N_2 adsorption isotherm

N_2 adsorption isotherm of surfactant modified and unmodified ZSM-5 samples are shown in Fig. 7. It can be seen

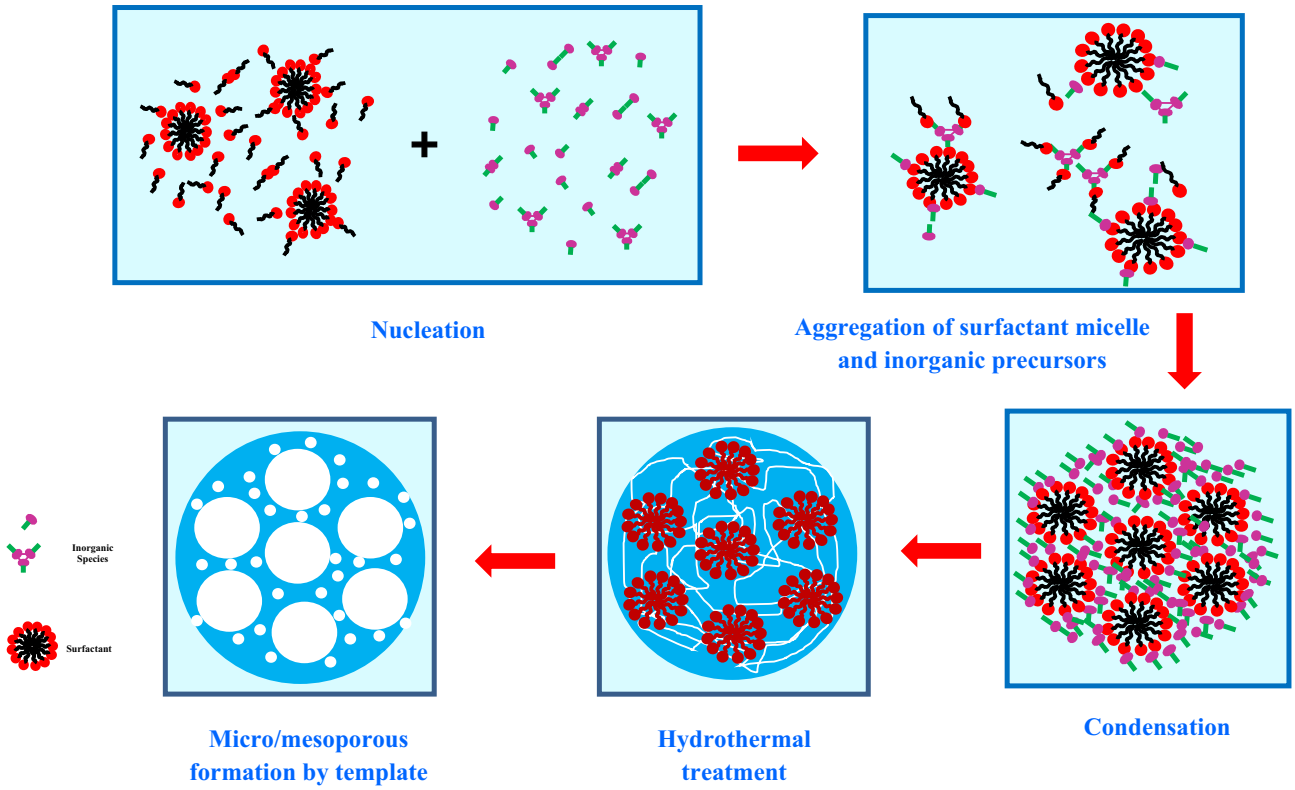

Scheme 1 Formation of hierarchical ZSM-5

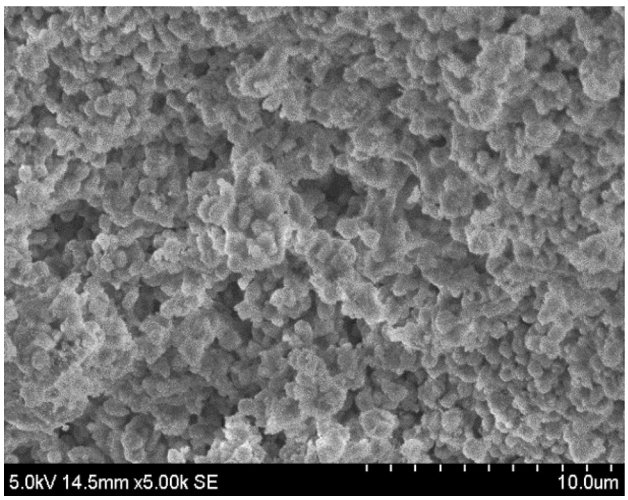

Fig. 5 SEM images of ZSM-5/HDSS sample

that the unmodified sample exhibits type I isotherm which is signature isotherm for microporous material. On the other hand, modified sample displays type IV isotherm, characteristics of mesoporous materials as defined by IUPAC nomenclature [26, 60, 61]. A steep uptake at low relative pressure ($P/P_0 = 0.5–0.9$), attribute to capillary condensation of N_2 in mesopores, further confirming the development of mesoporosity in the surfactant modified sample. The pore size distributions of the samples were evaluated by Barrett–Joyner–Halenda (BJH) model and is shown in Fig. 7(II). The estimated pore sizes for unmodified and modified sample are < 2 and 10–20 nm respectively. The results thus indicate that the additional mesoporosity was generated in ZSM-5 zeolite in the presence of HDSS surfactants.

The results of the thermogravimetric analysis of surfactant modified and unmodified ZSM-5 samples are given in Fig. 8. Both modified and unmodified samples displayed weight loss at 100 °C and 400–500 °C, due to the removal of physically adsorbed water molecules and decomposition of structure directing agent TPAOH from the sample respectively [62, 63]. An additional weight loss appeared in the range of 200–250 °C in the surfactant modified sample could be due to the degradation of the surfactant. High weight loss (22%) for surfactant modified sample together with the three DTA peak (Fig. 8b inset) can be taken as an evidence for the removal of both micro and mesotemplate from the zeolite framework. It can also be noted that the thermal stability of ZSM-5 zeolite is intact after modification with surfactant template.

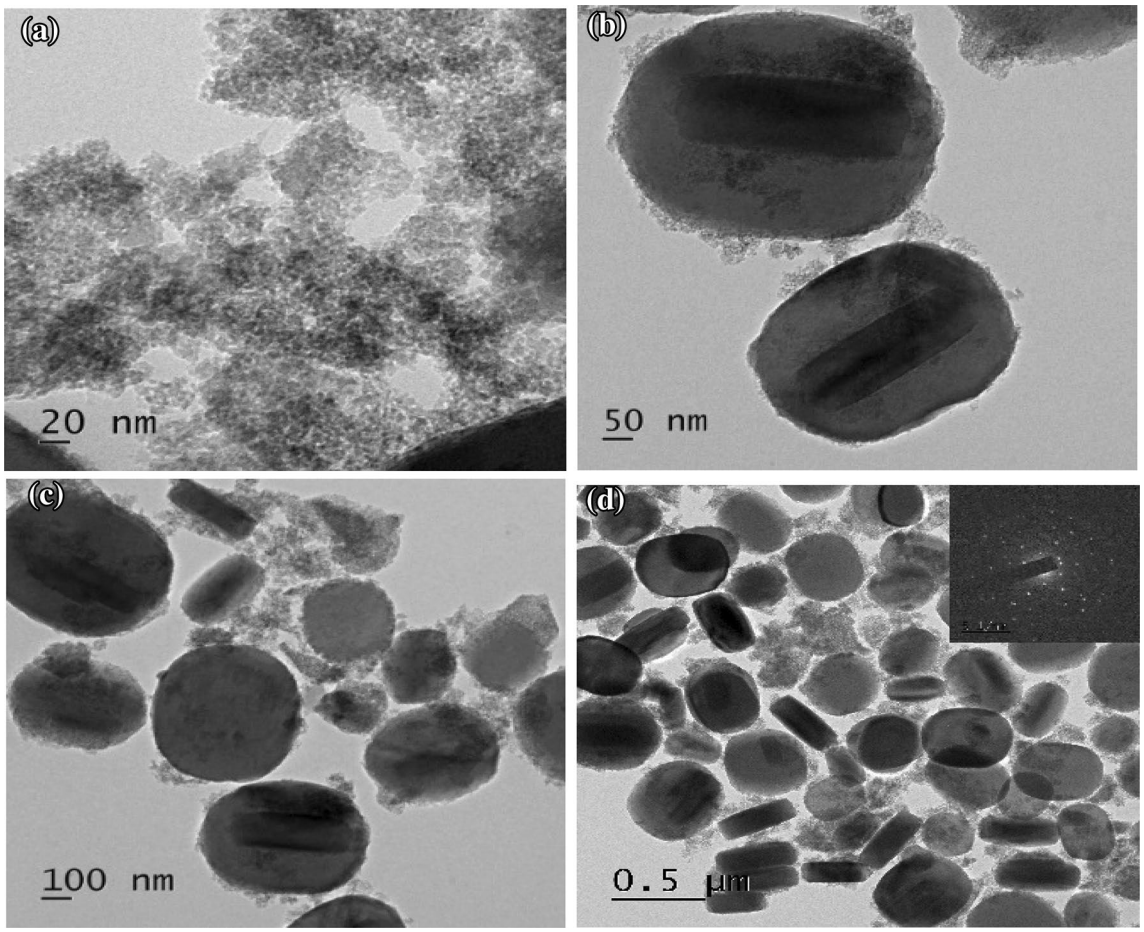

Fig. 6 TEM images of **a**–**d** ZSM-5/HDSS samples

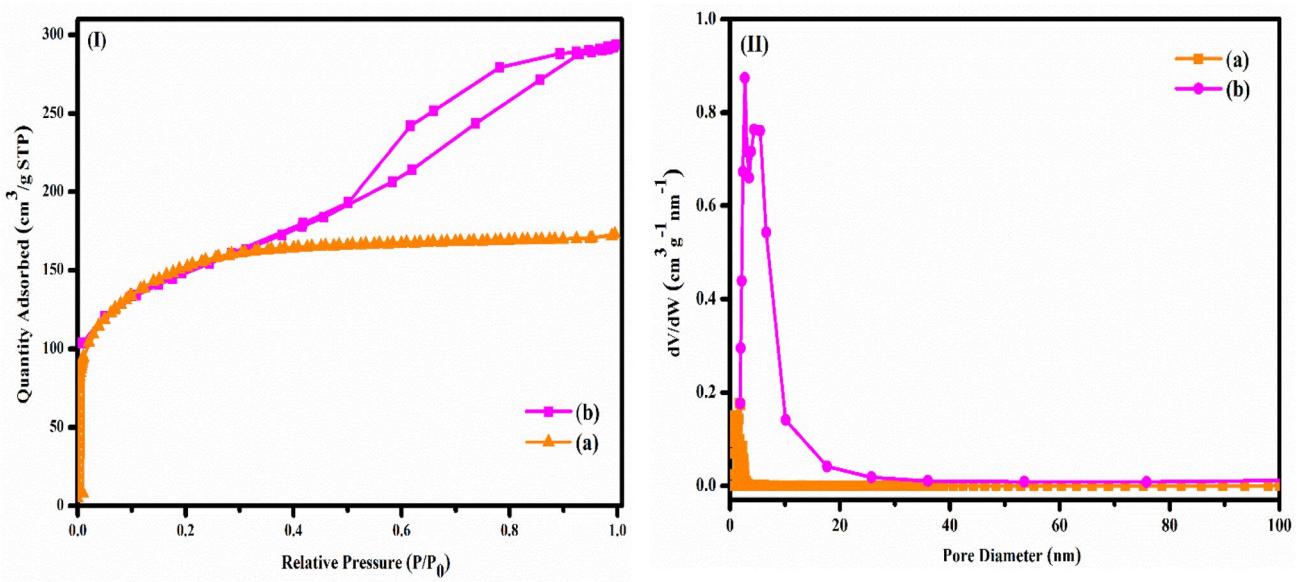

Fig. 7 N_2 adsorption isotherms of: **I** (a) ZSM-5, (b) ZSM-5/HDSS; Pore size distribution of: **II** (a) ZSM-5, (b) ZSM-5/HDSS

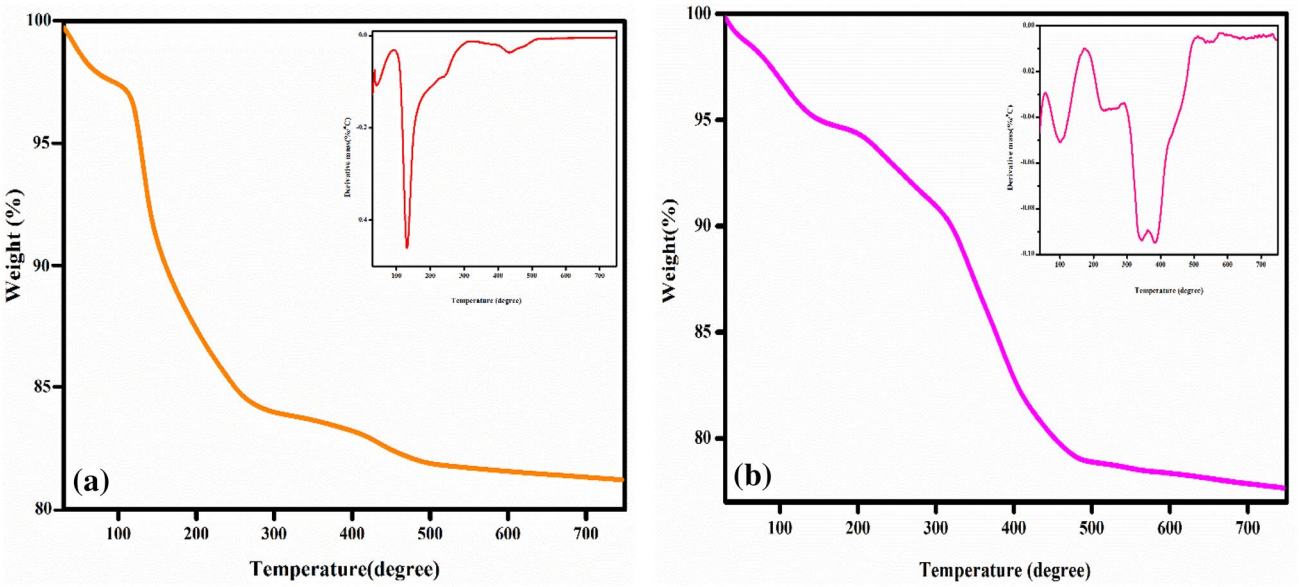

Fig. 8 TGA curve of: **a** ZSM-5, **b** ZSM-5/HDSS (DTG curves are given at the inset)

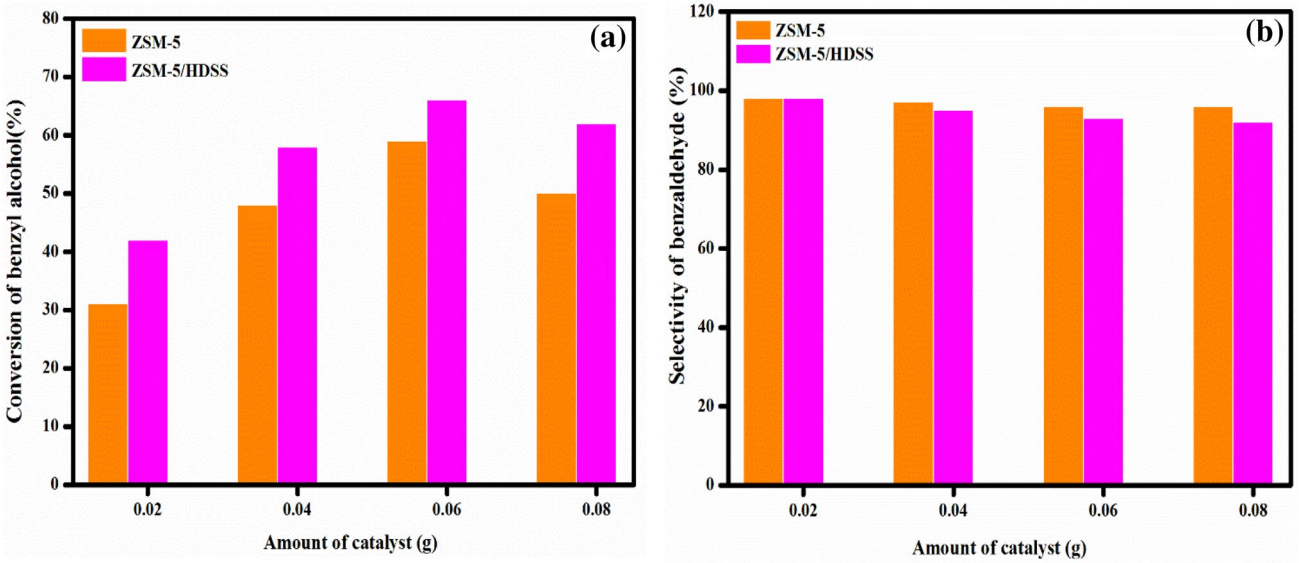

Fig. 9 Effect of catalyst amount on the oxidation of benzyl alcohol: **a** conversion of benzyl alcohol and **b** selectivity of benzaldehyde. Experimental conditions: benzyl alcohol—10 mmol, H_2O_2—15 mmol, temperature—90 °C, time—4 h

3.7 Catalytic activity for benzyl alcohol oxidation

The catalytic activities of the synthesized samples were tested using a model reaction: oxidation of benzyl alcohol using hydrogen peroxide as oxidant. Initially, we have varied the amount of catalyst from 0.02 to 0.08 g and its influence on benzyl alcohol conversion is shown in Fig. 9. The result shows that with increase in amount of catalyst, the conversion of benzyl alcohol also increases; attributed to the presence of more active sites on the catalyst. A further increase in the amount of catalyst does not result in any increase in conversion. Moreover, a decrease in selectivity has been observed at high amount of catalyst because of the further oxidation of benzyl alcohol to benzoic acid [64, 65]. Figure 10 shows the temperature effect on benzyl alcohol oxidation. It is evident from Fig. 10 that on increasing the temperature from 60 to 90 °C, the conversion of benzyl alcohol also increases by retaining the selectivity. However elevated temperature adversely affects the selectivity of benzyl alcohol and is attributed to the decomposition

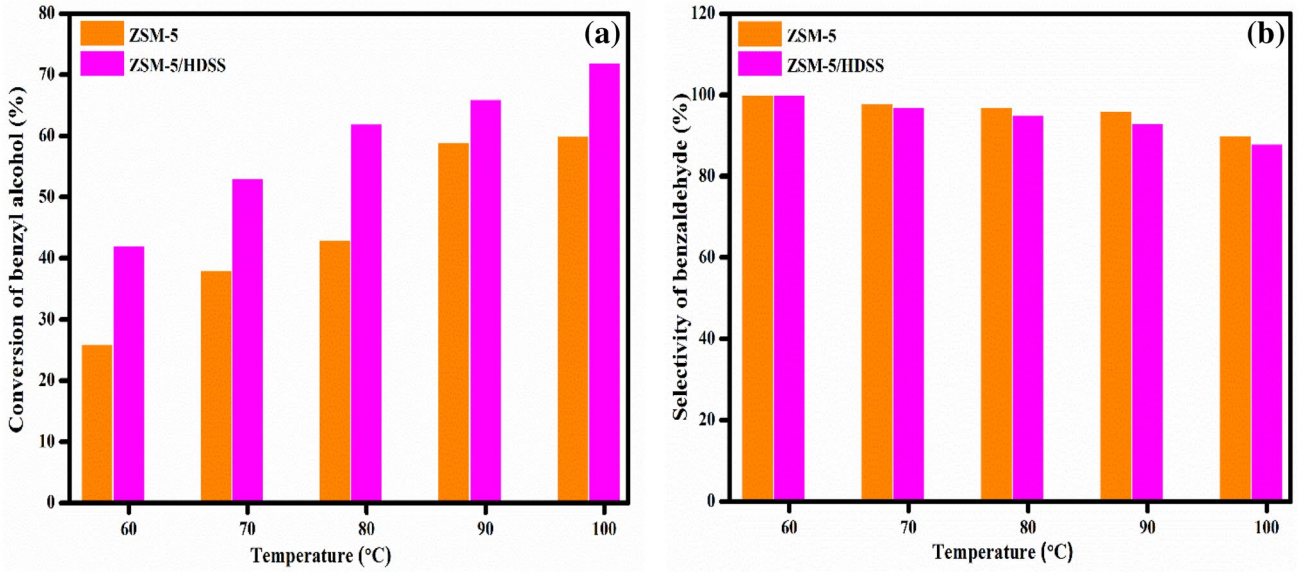

Fig. 10 Effect of the temperature on the oxidation of benzyl alcohol: **a** conversion of benzyl alcohol and **b** selectivity of benzaldehyde. Experimental conditions: benzyl alcohol—10 mmol, H_2O_2— 15 mmol, catalyst—0.06 g, time—4 h

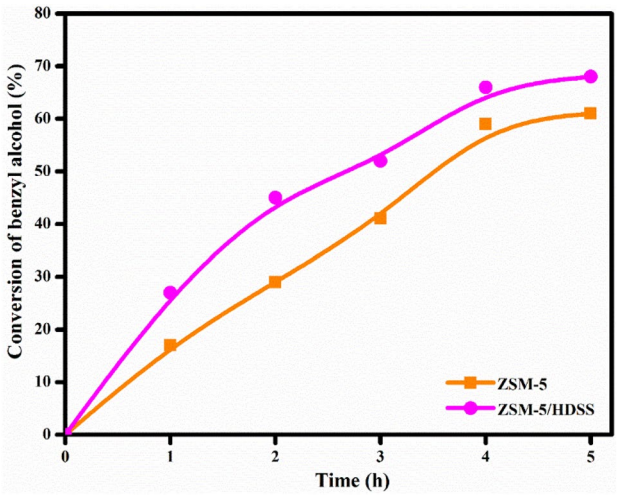

Fig. 11 Effect of the reaction time on the oxidation of benzyl alcohol: experimental conditions: benzyl alcohol – 10 mmol, H_2O_2—15 mmol, temperature—90 °C, catalyst—0.06 g

of hydrogen peroxide at high temperature. The result thus indicates that 90 °C is ideal for the conversion of benzyl alcohol using surfactant modified ZSM-5 catalyst. We have also examined the conversion and selectivity of benzyl alcohol with different reaction times (Fig. 11). It is evident that the conversion of benzyl alcohol increases with reaction time and reaches maximum in 4 h; thereafter it becomes stable. This is could be due to the progressive consumption of H_2O_2 for oxidation of benzyl alcohol or due to its self-decomposition. The maximum conversion was obtained during the first 4 h. A comparison of the catalytic activity of modified

Table 1 Reusability of hierarchical ZSM-5 catalyst for oxidation of benzyl alcohol

Recycle	ZSM-5 Conversion of BzOH (%)	ZSM-5/HDSS Conversion of BzOH (%)
1	56	63
2	54	60
3	52	59

Experimental conditions: benzyl alcohol—10 mmol, H_2O_2—15 mmol, temperature—90 °C, catalyst—0.06 g, time—4 h

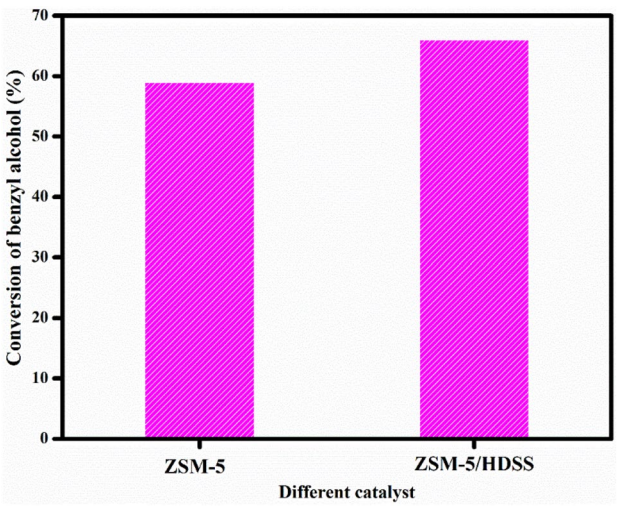

Fig. 12 Effect of different catalyst on the oxidation of benzyl alcohol: experimental conditions: Benzyl alcohol—10 mmol, H_2O_2—15 mmol, temperature—90 °C, catalyst—0.06 g, time 4—h

and unmodified sample is depicted in Fig. 12. The higher catalytic activity for surfactant modified zeolite could be due to additional porosity in sample. Finally, we have tested the reusability of zeolite catalysts made with the assistance of surfactants. The catalysts displayed high reusability even after three recycle (Table 1).

4 Conclusion

Hierarchical ZSM-5 catalyst was successfully developed using a novel soft mesotemplate HDSS. The unique pentasil structure of the catalyst was confirmed by XRD, FT-IR and NMR analysis. The surfactant templated ZSM-5 catalyst possesses micro and mesopores which was confirmed from N_2 adsorption and TEM techniques. The HDSS modified catalyst thus has better mass transfer and consequently accelerates the rate of large molecular reactions: liquid phase oxidation of benzyl alcohol with H_2O_2 as an oxidant. We have also optimized experimental conditions such as the catalyst amount, temperature and time for the oxidation of benzyl alcohol. Our studies show that high benzyl alcohol conversion (63%) was achieved for 0.06 g of catalyst at 90 °C for 4 h. The recycle studies indicates that catalysts derived through surfactant mediated process exhibits better reusability and their activity was retained even after three recycle.

Acknowledgements The authors thank the Science & Engineering Research Board, New Delhi, India, for funding this research. [File No: SR/S1/OC-40/2011 dated 15/5/2012]

Data Availability The raw/processed data required to reproduce these findings cannot be shared at this time as the data also forms part of an ongoing study.

Compliance with ethical standards

Conflict of interest The authors declare that they have no conflict of interest.

Reference

1. F. Adam, W.T. Ooi, Appl. Catal. A **445-446**, 252–260 (2012)
2. G.C. Behera, K.M. Parida, Appl. Catal. A **413-414**, 245–253 (2012)
3. Y. Perez, R. Ballesteros, M. Fajardo, I. Sierra, I. del Hierro, J. Mol. Catal. A **45**, 352 (2012)
4. S. Ajaikumar, A. Pandurangan, J. Mol. Catal. A **35**, 290 (2008)
5. A. Jia, L.L. Lou, C. Zhang, Y. Zhang, S. Liu, J. Mol. Catal. A **123**, 306 (2009)
6. I.A. Shibley Jr., K.E. Amaral, D.J. Aurentz, R.J.J. McCaully, Chem. Educ. **87**, 1351–1354 (2010)
7. N.J. Hill, J.M. Hoover, S.S. Stah, J. Chem. Educ. **90**, 102–105 (2013)
8. F. Sadri, A. Ramazani, A. Massoudi, M. Khoobi, R. Tarasi, A. Shafiee, V. Azizkhani, L. Dolatyari, S.W. Joo, Green Chem. Lett. Rev. **7**, 257–264 (2014)
9. R. Noyori, M. Aoki, K. Sato, ChemCommun **34**, 1977–1986 (2003)
10. T. Mallat, A. Baiker, Chem. Rev. **104**, 3037–3058 (2004)
11. M. Besson, P. Gallezot, Catal. Today **57**, 127–141 (2000)
12. N. Dimitratos, J.A. Lopez-Sanchez, D. Morgan, A. Carley, L. Prati, G.J. Hutchings, Catal. Today **122**, 317–324 (2007)
13. Y. Chen, H. Lim, Q. Tang, Y. Gao, T. Sun, Q. Yan, Y. Yang, Strategic innovation and new product development in family firms: An empirically grounded theoretical framework. Appl. Catal. A **380**(2), 55–65 (2010)
14. M.A. Snyder, M. Tsapatsis, Angew. Chem. Int. Ed. **46**, 7560–7573 (2007)
15. A. Corma, Chem. Rev. **97**, 2373–2419 (1997)
16. Y. Tao, H. Kanoh, L. Abrams, K. Kaneko, Chem. Rev. **106**, 896–910 (2006)
17. A. Corma, J. Catal. **216**, 298–312 (2003)
18. T. Bein, Chem. Mater. **8**, 1636–1653 (1996)
19. M.E. Davis, Nature **417**, 813–821 (2002)
20. C.S. Cundy, P.A. Cox, Chem. Rev. **103**, 663–701 (2003)
21. A. Corma, Chem. Rev. **95**, 559–614 (1995)
22. K.L. Yeung, W. Han, Catal. Today **236**, 182–205 (2014)
23. S.H. Kareem, I.H. Ali, M.G. Jalhoom, Am. J. Environ. Sci. **10**, 48–60 (2014)
24. S. Aguado, A.C. Polo, M.P. Bernal, J. Coronas, J. Santamaría, J. Membr. Sci. **240**, 159–166 (2004)
25. A. Hauer, S. Fischer, E. Lävemann, Thermal applications of zeolite/water adsorption processes, in *Fundamentals of adsorption. The kluwer international series in engineering and computer science*, ed. by M.D. LeVan (Springer, Boston, 1996)
26. S. Narayanan, J. Judith Vijaya, S. Sivasanker, S. Yang, L. John Kennedy, Chin. J. Catal. **35**, 1892–1899 (2014)
27. Z.L. Hua, J. Zhou, J.L. Shi, Chem. Commun. **47**, 10536–10547 (2011)
28. Y. Liu, T.J. Pinnavaia, J. Am. Chem. Soc. **12**, 3179–3190 (2002)
29. F.S. Xiao, L. Wang, C. Yin, K. Lin, Y. Di, J. Li, R. Xu, D.S. Su, R. Schlogl, T. Yokoi, T. Tatsumi, Angew. Chem. Int. Ed. **45**, 3090–3093 (2006)
30. V. Valtchev, M. Smaihi, A.C. Faust, L. Vidal, Angew. Chem. Int. Ed. **42**, 2782–2785 (2003)
31. Y.S. Tao, H. Kanoh, K. Kaneko, J. Am. Chem. Soc. **125**, 6044–6045 (2003)
32. A.J.J. Koekkoek, H.C. Xin, Q.H. Yang, C. Li, E.J.M. Hensen, Microporous Mesoporous Mater. **145**, 172 (2011)
33. S.S. Kim, J. Shah, T.J. Pinnavaia, Chem. Mater. **15**, 1664–1668 (2003)
34. Y.S. Tao, H. Kanoh, Y. Hanzawa, K. Kaneko, Colloids Surf. A **241**, 75–80 (2004)
35. M. Choi, H.S. Cho, R. Srivastava, C. Venkatesan, D.H. Choi, R. Ryoo, Nat. Mater. **5**, 718–723 (2006)
36. J.H. Yang, S.X. Yu, H.Y. Hu, Y. Zhang, J.M. Lu, J.Q. Wang, D.H. Yin, Chem. Eng. J. **166**, 1083 (2011)
37. L.F. Wang, Z. Zhang, C.Y. Yin, Z.C. Shan, F.S. Xiao, Microporous Mesoporous Mater. **131**, 58 (2010)
38. Y. Wang, H. Tao, C. Li, J. Ren, G. Lu, J. Solid State Chem. **184**, 1820–1827 (2011)
39. J. Shi, J. Jin, X. Zhang, Y. Li, H. Li, Y. Cui, Q. Chen, L. Li, J. Gu, W. Zhao, Chem. Eur. J. **18**, 16549–16555 (2012)
40. M. Krishnamurthy, M.S.M. Kamil, C.K. Krishnan, Microporous Mesoporous Mater. **221**, 23–31 (2016)
41. Y. C.Yin, F. Wei, Y. Wang, Chen, Mater Lett **98**, 194–196 (2013)
42. B. Liu, C. Li, Y. Ren, Y. Tan, H. Xi, Y. Qian, Chem. Eng. J. **210**, 96–102 (2012)
43. D. Xu, S. Che, J. Feng, Dalton Trans. **43**, 3612–3617 (2014)

44. E.J.M. Hensen, X. Zhu, R. Rohling, G. Filonenko, B. Mezari, J.P. Hofmann, S. Asahina, Chem. Commun. **50**, 14658–14661 (2014)
45. Z. Zhu, M. Liu, J. Li, W. Jia, M. Qin, Y. Wang, K. Tong, H. Chen, RSC Adv. **5**, 9237–9240 (2015)
46. J.M. Gómez, E. Díez, A. Rodríguez, M. Calvo, Microporous Mesoporous Mater. (2018). https://doi.org/10.1016/j.micromeso.2018.05.029
47. J.M. Gómez, E. Díez, I. Bernabe, Catal. Commun. **78**, 55–58 (2016)
48. R. Ling, W. Chen, J. Hou, Particuology **36**, 190–192 (2018)
49. T. Haixiang, Y. Hong, Z. Yanhui, R. Jiawen, L. Xiaohui, W. Yanqin, L. Guanzhong, J. Mater. Chem. A. **1**, 13821–13827 (2013)
50. Q. Wang, S. Xu, J. Chen, Y. Wei, J. Li, D. Fan, Z. Yu, Y. Qi, Y. He, S. Xu, C. Yuan, Y. Zhou, J. Wang, M. Zhang, B. Su, Z. Liu, RSC Adv. **4**, 21479–21491 (2014)
51. J. Jiang, C. Duanmu, Y. Yang, X. Gu, J. Chen, Powder Technol. **251**, 9–14 (2014)
52. Z. Wang, P. Dornath, C.C. Chang, H. Chen, W. Fan, Microporous Mesoporous Mater. **181**, 8–16 (2013)
53. H. Chen, Y. Wang, C. Sun, X. Wang, C. Wang, Catal. Commun. **112**, 10–14 (2018)
54. R. Srivastava, M. Choi, R. Ryoo, Chem. Commun. **43**, 4489–4491 (2006)
55. J.F. Silva, E.D. Ferracine, D. Cardoso, Appl. Sci. **8**, 1299 (2018)
56. R. Chal, T. Cacciaguerra, S.V. Donk, C. Gerardin, Chem. Commun. **46**, 7840–7842 (2010)
57. Y. Maa, J. Hu, L. Jia, Z. Li, Q. Kan, S. Wu, Mater. Res. Bull. **48**, 1881–1884 (2013)
58. H. Chen, Y. Wang, C. Sun, X. Wang, Catal. Commun. **112**, 10–14 (2018)
59. X. Wang, H. Chen, F. Meng, F. Gao, C. Sun, L. Sun, S. Wang, L. Wang, Microporous Mesoporous Mater. **243**, 271–280 (2017)
60. S. Han, Z. Wang, L. Meng, N. Jiang, Mater Chem Phys. 1–6 (2016)
61. G. Leofantia, M. Padovanb, G. Tozzolac, B. Venturellic, Catal. Today **41**, 207–219 (1998)
62. Y. Ma, J. Hu, L. Jia, Z. Li, Q. Kan, S. Wu, Mater. Res. Bull. **48**, 1881–1884 (2013)
63. Y. Zhang, C. Jin, J. Solid State Chem. **184**, 1–6 (2011)
64. S. Narayanan, J. Judith Vijaya, S. Sivasanker, L. John, S.K. Kennedy, Jesudoss, Powder Technol. **274**, 338–348 (2015)
65. A. Jia, L.L. Lou, C. Zhang, Y. Zhang, J. Mol. Catal. A **306**, 123–129 (2009)